



# NUMERICAL STUDY OF AGGREGATE EFFECTS ON THE STRENGTH OF LIGHT CONCRETE

Miryuk O. A., Oleinik A. I. and Akhmedov K. M.

Rudny Industrial Institute let Oktyabrya Street, Rudny, Kostanay Region, Kazakhstan

E-mail: [psm58@mail.ru](mailto:psm58@mail.ru)

## ABSTRACT

The article represents the results of lightweight concrete's composition designing by numerical methods. The study is aimed at finding rational aggregate particles packing that provides the highest mechanical characteristics of the composite material. Numerical simulation uses the finite element method. To simplify a calculation scheme, the study was carried out in a flat format. Models with regular aggregate particles of spherical and cylindrical shape have been investigated. The advantage of a two-component model built on the fractal principle of a triangle and containing up to 70% of aggregate particles has been proven. The model of aggregate distribution according to the type of an equilateral triangle provides minimal stresses and deformations inside the composite material. To ensure the mechanical resistance of the composite material, the rounded shape of granules is preferable compared to quasi-cylindrical particles. Under a regular multi-row distribution of rounded granules, the model containing particles with diameter from 6 to 8 mm is characterized by a minimum concentration of normal and shear stresses. The results of numerical simulation are consistent with experimental studies of lightweight alkaline silicate concrete based on porous granular aggregate.

**Keywords:** lightweight concrete, porous aggregate, finite element method, plane stress condition, regular aggregate packing.

## 1. INTRODUCTION

An important advantage of concrete is a wide possibility of regulating its composition and structure by changing components of the molding sand. The use of porous aggregate makes it possible to obtain lightweight concretes characterized by low density and heat-shielding properties. The use of lightweight concrete provides reduction in products' mass, in the consumption of steel reinforcement, and reduction in the cost of construction; it allows implementing complex architectural and space-planning solutions [1-3]. Lightweight concretes' best operating practices confirmed their operational reliability. Development, improvement of quality and expansion of the scope of lightweight concretes is a trend in the modern construction.

Lightweight concrete is a composite material where porous aggregate particles are held by a matrix substance. For most concretes, the matrix is a hardened cement stone. Lightweight concrete aggregate is the dominant component of the molding sand; it is distinguished by a variety of shapes, sizes, and surface conditions. This is due to the wide raw material base for its obtaining. Geometric and structural characteristics of aggregate significantly affect technological properties of the concrete mixture, and concrete's quality. The content of aggregate in the concrete mixture also determines cement consumption, which affects the cost and durability of concrete.

When creating lightweight concretes on porous aggregates, it is important to optimize the structure due to the orderliness of packing elements. Therefore, the search for the optimal aggregate particles packing in concrete is of great relevance. Importance of this problem increases with the use of new types of aggregate [4-7], utilization of technogenic materials [8-14], and development of modern building technologies [15, 16].

To optimize the structure of concrete, computer modeling is used. Numerical research methods are based on the principles of fractal geometry. The geometry of fractals makes it possible to model geometric and physical systems with partially ordered structures [17, 18].

The objective of the work is to compile and study a model of lightweight concrete based on aggregate of various configurations. The study is aimed at finding a solution providing the highest mechanical characteristics of the composite material.

Developments in optimizing the structure of concrete are often aimed at numerical studies of systems with rounded aggregate particles [19-21]. In this work, particles of spherical and cylindrical shapes have been studied.

## 2. MATERIALS AND METHODS OF INVESTIGATION

The object of the study has been a numerical model of lightweight concrete with porous aggregate. The study of the model has been carried out by the finite element method [22, 23] using the Lira CAD software. A flat element 10 mm thick, cut from a concrete sample 100 × 100 × 100 mm in size, has been studied as a typical model. To simplify numerical calculations, the spherical shape of aggregate particles is indicated as a circle. Aggregate modulus of elasticity is  $E_f = 2000$  MPa, for the matrix substance is  $E_b = 10000$  MPa. Practically non-deformable steel plate imitating a stamp is installed in the upper part of the model. The base nodes are fixed in all the directions. The model is designed for a reduced unit distributed load of unit intensity, which makes it possible to switch to real loads using a scaling factor. The results of the numerical study were tested on a material object - lightweight alkaline silicate concrete. Porous glass-ceramic granular material was used as aggregate [24, 25]. The lightweight concrete matrix is



represented by liquid-glass binder containing technogenic fillers (for example, cullet, solid fuel ash, and others). The choice of the cementless binder is due to the high adhesive ability and low energy consumption of liquid glass materials. Molding sands were obtained by mixing the components in the following order: a technogenic component (45-55%) was added to liquid glass (density 1350 kg/m<sup>3</sup>), then porous filler was introduced into the resulting suspension. Samples measuring 100 x 100 x 100 mm, made from the molding sand, were subjected to heat treatment. Strength properties of concretes were determined by testing samples on a hydraulic press. The macrostructure of concrete was studied by a visual method.

### 3. RESULTS AND DISCUSSIONS

#### 3.1 Study of Numerical Models of Lightweight Concrete

To study the influence of matrix content on strength properties of a composite material, a multi-row packing of aggregate of rounded particles (granules) was considered. The matrix material has higher strength characteristics, modulus of elasticity, ultimate compressive and tensile strength compared to the aggregate material. The intercontact space between the particles is occupied by the matrix and is approximately 1 mm.

There is a variant of three-component packing according to the principle of built-in squares (structure I), at the tops of which are grains of different diameters in Figure-1. The size of the diameters of particles ensures the same gaps between the grains. The deformation fields along the horizontal - X, vertically - Z, isofields of normal and tangential stresses  $\sigma_x$ ,  $\sigma_z$ ,  $\tau_{xz}$  have been obtained. Analysis of the typical stress distribution in the  $\sigma_x$  model shows that the normal stress fields are inhomogeneous and have stress concentrations along the grain boundaries, with the maximum stresses occurring in the matrix.

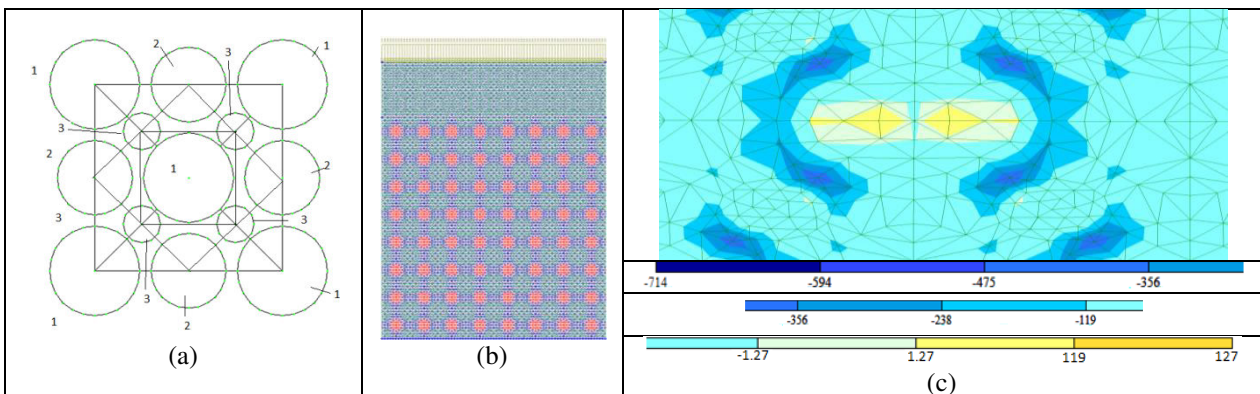


**Figure-1.** Three-component grain packing model with repeated squares: a) structure with grain diameters as follows: 1 - 12 mm, 2 - 10 mm, 3 - 5 mm; b) finite element model; c) normal stress isofields for  $\sigma_x$ .

Structure II is characterized by aggregate packing according to the fractal principle of similarity distribution by type of an equilateral triangle (Figure-2). There are

eight similar triangles in a typical cell, which determines denser packing of grains and provides increase in strength properties of the combined model.

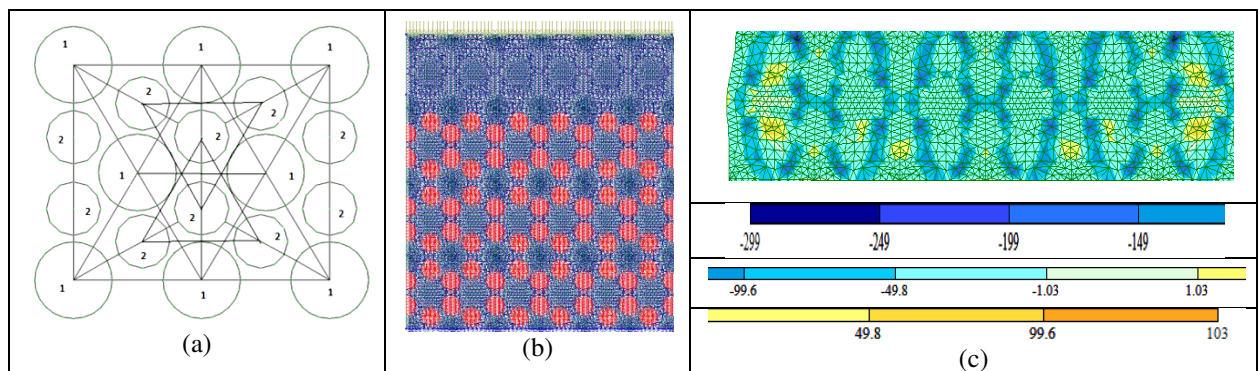


**Figure-2.** Two-component grain packing model with repeating triangles: a) structure with grain diameters: 1 - 10 mm, 2 - 8 mm; b) finite element model; c) normal stress isofields for  $\sigma_x$ .



Regular two-row packing model has universal properties: each element has a main core and additional annular sections (Figure-3). By varying values of the modulus of elasticity of structure's elements, it is possible to obtain results for the aggregate with a diameter of up to 14 mm and different content of the matrix.

Three variants of structures (III, IV, and V) were calculated in the two-row packing model. Structure III is: identical individual elements with variations in their diameters. Structure IV is: one of the alternating elements

(aggregate) has the same modulus of elasticity as the matrix. Structure V is: the same values of the modulus of elasticity inside each particle; presence of strong shells around the cores of particles with  $E_s=20000$  MPa; the matrix is characterized by  $E_b=10000$  MPa.

Results of the study of models I - V for two values of the aggregate deformation modulus of  $E_i=1000$  MPa,  $E_i=100$  MPa with the matrix deformation modulus  $E_b=10000$  MPa are shown in Tables 1 and 2.

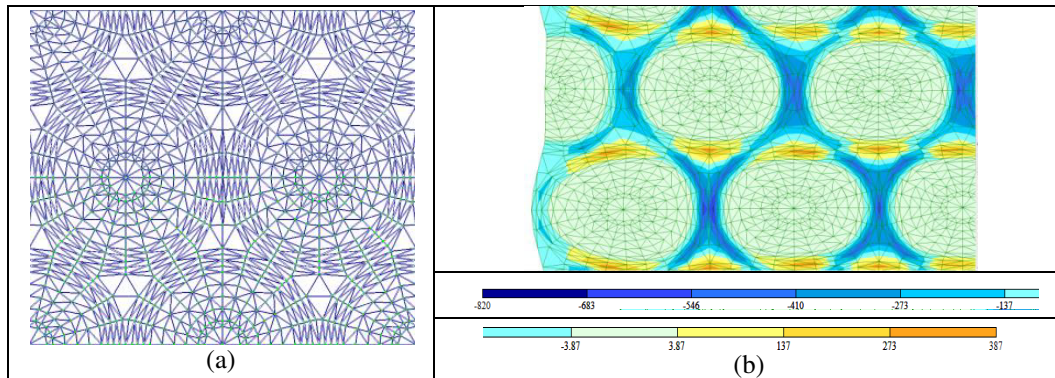


**Figure-3.** Regular two-row grain packing model with partition into finite elements: a) structure; b) typical distribution of normal stresses  $\sigma_z$ .

**Table-1.** Results of numerical studies of various aggregate packing schemes.

| Structure | $E_b$ , MPa    | $E_i$ , MPa    | X, mm  | Z, mm  | $-\sigma_x$ , MPa | $+\sigma_x$ , MPa |
|-----------|----------------|----------------|--------|--------|-------------------|-------------------|
| I         | $1 \cdot 10^4$ | $1 \cdot 10^4$ | 0.0080 | 0.0468 | 3.37              | 0.452             |
|           | $1 \cdot 10^4$ | $1 \cdot 10^2$ | 0.0260 | 0.1040 | 8.34              | 0.159             |
| II        | $1 \cdot 10^4$ | $1 \cdot 10^4$ | 0.0057 | 0.0277 | 2.38              | 0.338             |
|           | $1 \cdot 10^4$ | $1 \cdot 10^2$ | 0.0121 | 0.0452 | 2.95              | 0.990             |
| III       | $1 \cdot 10^4$ | $1 \cdot 10^4$ | 0.0091 | 0.0425 | 4.67              | 0.597             |
|           | $1 \cdot 10^4$ | $1 \cdot 10^2$ | 0.0276 | 0.0852 | 6.97              | 2.590             |
| IV        | $1 \cdot 10^4$ | $1 \cdot 10^4$ | 0.0069 | 0.0354 | 5.36              | 0.148             |
|           | $1 \cdot 10^4$ | $1 \cdot 10^2$ | 0.0166 | 0.0637 | 11.10             | 0.727             |
| V         | $1 \cdot 10^4$ | $1 \cdot 10^4$ | 0.0082 | 0.0360 | 5.46              | 1.120             |
|           | $1 \cdot 10^4$ | $1 \cdot 10^2$ | 0.0190 | 0.0620 | 7.46              | 3.300             |

**Table-2.** Calculated rates of mechanical properties for various aggregate packing schemes.

| Structure | Aggregate content, % | $-\sigma_z$ , MPa | $+\sigma_z$ , MPa | $-\tau_{xz}$ , MPa | $+\tau_{xz}$ , MPa | $\varepsilon_z \cdot 10^{-4}$ | $E_p \cdot 10^3$ , MPa |
|-----------|----------------------|-------------------|-------------------|--------------------|--------------------|-------------------------------|------------------------|
| I         | 70                   | 2.79              | 1.020             | 0.975              | 0.626              | 4.68                          | 3.80                   |
|           | 70                   | 5.11              | 1.750             | 2.070              | 2.000              | 10.40                         | 2.50                   |
| II        | 70                   | 4.75              | 0.522             | 0.889              | 0.106              | 2.77                          | 14.50                  |
|           | 70                   | 7.82              | 2.490             | 1.350              | 1.270              | 4.52                          | 15.30                  |
| III       | 70                   | 4.17              | 0.651             | 2.010              | 0.952              | 4.25                          | 6.50                   |
|           | 70                   | 7.31              | 2.810             | 4.280              | 2.310              | 8.52                          | 6.13                   |
| IV        | 70                   | 6.21              | 0.443             | 2.020              | 0.964              | 3.54                          | 13.00                  |
|           | 70                   | 13.00             | 1.970             | 4.250              | 2.170              | 4.41                          | 15.10                  |
| V         | 70                   | 4.65              | 0.978             | 1.610              | 1.150              | 3.60                          | 8.30                   |
|           | 70                   | 7.32              | 3.000             | 3.480              | 2.320              | 6.20                          | 8.20                   |

The reduced modulus of elasticity of the model ( $E_p$ ) is calculated for a plane stress state. Characteristic feature of the deformation for the structures under study is development of significant concentrations of compressive stresses along the contour of the largest grains and appearance of significant tensile stresses inside these grains. For structure II, under the same load, the most uniform distribution of normal stresses was obtained. This scheme corresponds to the minimum levels of stress and strain intensity, while the elastic modulus reaches the maximum. This scheme can be considered close to the optimal variant.

Analysis of distributions of stress isofields ( $\sigma_z$ ,  $t/m^2$ ) in Figure-4 and the characteristics in Figures 5 and 6 revealed a nonlinear dependence of the stress intensity on the granule diameter.

When granule diameters are small (Figure-4 a-b), the external load on the material is taken up by the matrix located vertically between the grains. In this case, the matrix substance above the granule and under the granule does not participate in the work.

When granule diameters are average (Figure-4 c-d), the normal compressive stresses are distributed almost evenly over the core shell around the granule, and the maximum volume of the matrix is involved in the work.

Tensile stresses develop in the shell around the granule for large granules (Figure-4 e-f); it negatively affects composite material's operation.

To maximize the use of matrix binder reserves, an optimal area has been identified corresponding to a granule diameter of 6-8 mm and matrix content in the material of at least 30 %. At the same time, the concentration of normal and shear stresses is minimal. There is decrease in elasticity modulus of granules to the limiting values (below 10-100 MPa), corresponding to voids as aggregate; it has little effect on the nature of the revealed regularities. Consequently, the main role in the stress-strain state of composite materials is played by matrix substance configuration, determining the ability to redistribute forces between the elements of the structure.

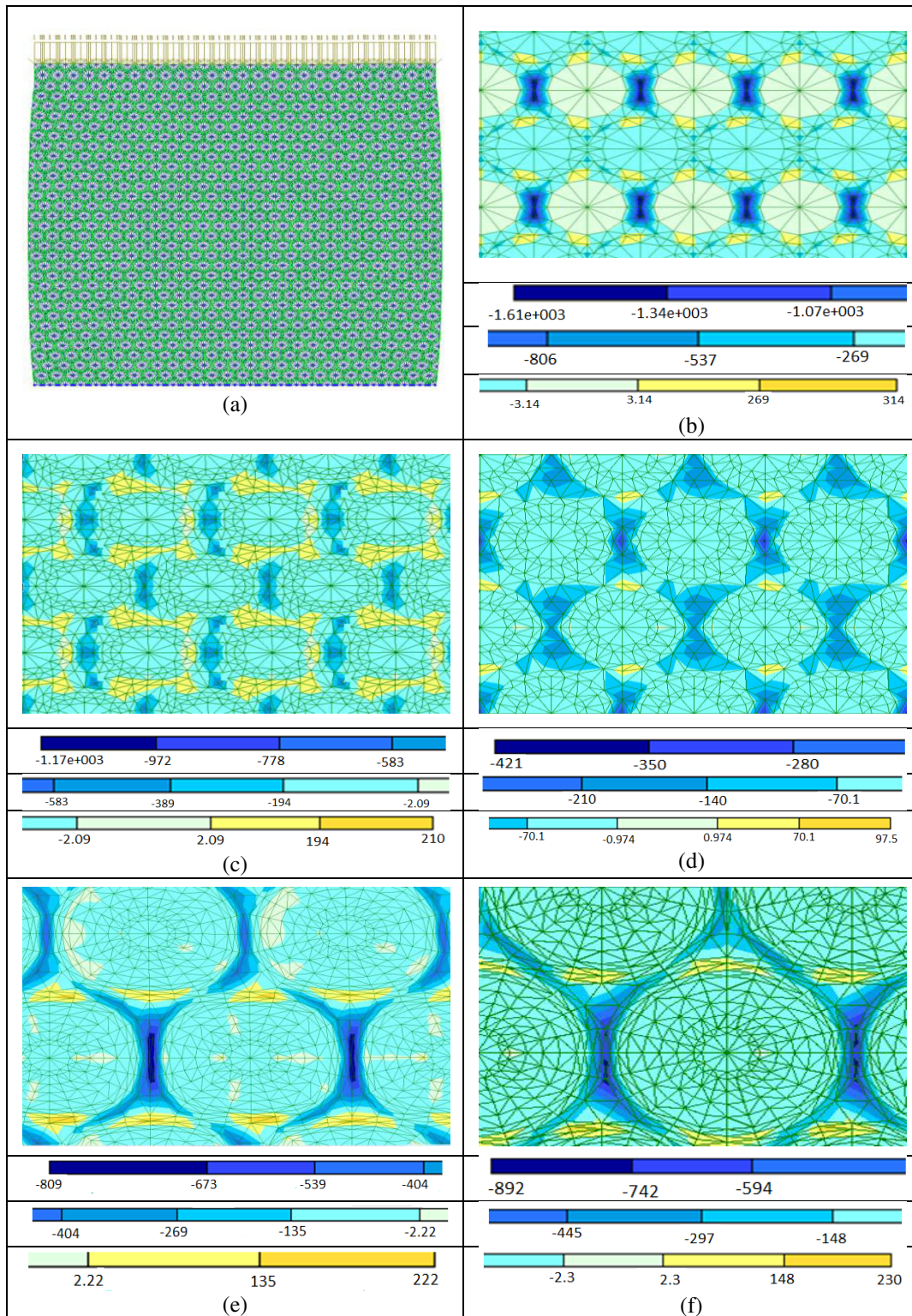


**Figure-4.** Isofields of normal stresses  $\sigma_z$  ( $t/m_2$ ) of models with different diameters of aggregate particles: a) 3 mm; b) 3 mm; c) 6 mm; d) 8 mm; e) 10 mm; f) 12mm.

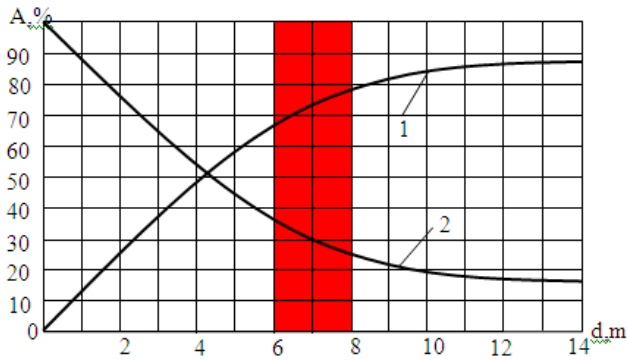


**Figure-5.** Effect of aggregate granule’s diameter (d, mm) on the component content (A,%) in the composite material model: 1- is granule’s content; 2- is the content of the matrix.

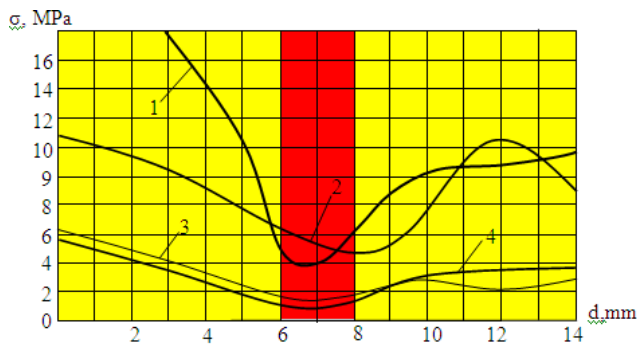


**Figure-6.** Influence of the diameter of aggregate granule (d, mm) on the stress concentration in the composite material model: 1-  $\sigma_z(-)$ ; 2-  $\sigma_x$ ; 3- z (+); 4-  $\tau_{max}$  (yellow is an area with stress concentration in the matrix above the limit values).

The molding technology makes it possible to create aggregate in the form of short cylindrical or nearly cylindrical grains. It is of interest to study stress and strain fields in models with quasi-cylindrical particles. Figures 7 and 8 show the results of studying two schemes of the

model with quasi-cylindrical particles (Figure-7). Arrangement of cylindrical particles in the parallel plane of the model and perpendicular to the plane is taken into account. In the latter case, the particles are projected onto the plane in the form of circles.

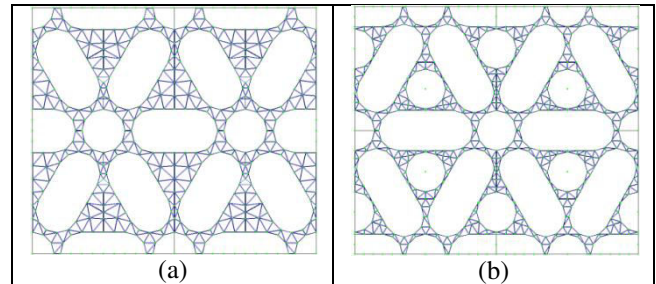


**Figure-7.** The nature of distribution of cylindrical aggregate particles in the composite material model: a) aggregate’s diameter is 7 mm, length is 14 mm, and content is 56%; b) aggregate’s diameter is 7 mm, length is 17 mm, content is 82%.

Analysis of normal stress isofields shows that tensile stresses develop along the side surfaces of cylindrical particles (Figure-8 a-b), causing cracking. Similar to the model containing round grains, the content of the matrix is of great importance. Tensile stresses combined with normal ultimate compressive stresses lead to flattening of the aggregate particles (Figure 8 c-d) under a very dense packing of quasi-cylindrical particles (Figure-7b). Taking into account the noted phenomena, the rounded shape of grains is more preferable. When using cylindrical particles, it is advisable to observe the ratio "diameter: length", equal to 1:2. In this case, the content of matrix must be at least 40 %. If these conditions are violated, flattening of some aggregate grains and development of accidental destruction are likely.

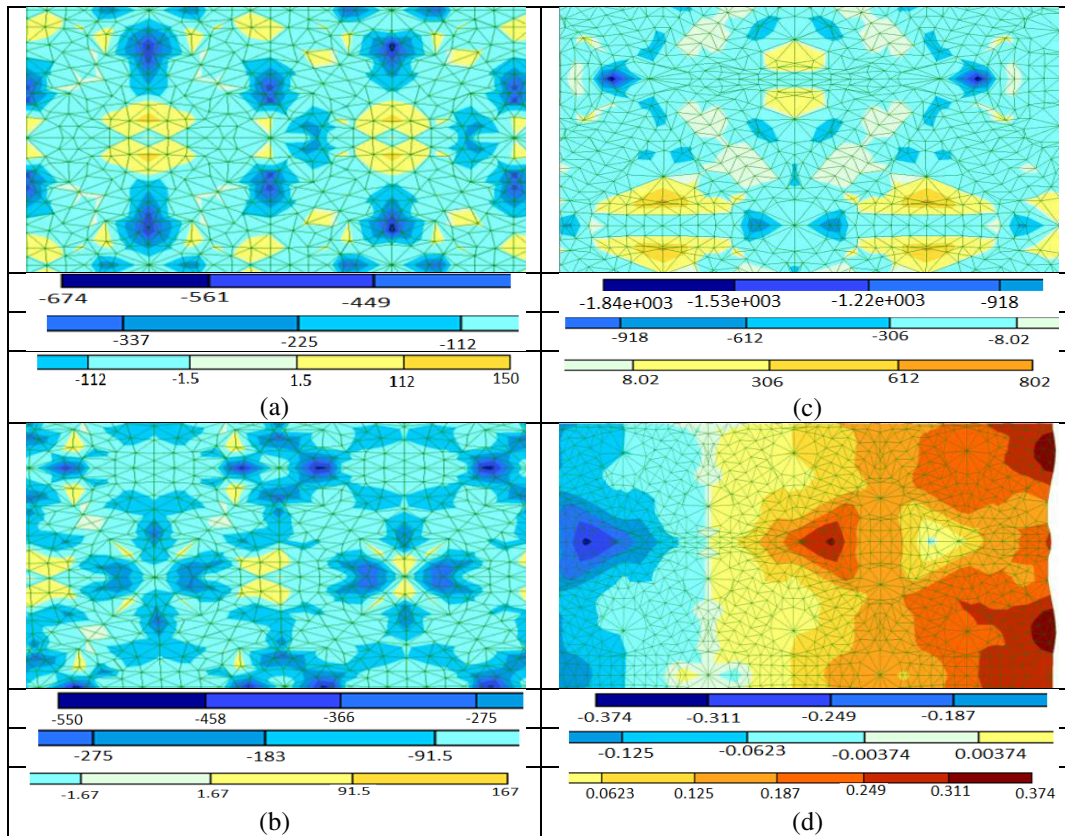


**Figure-8.** Stress isofields in the composite material model: a) normal stresses,  $\sigma_x$ ,  $t/m^2$ , scheme 1; b) normal stresses,  $\sigma_z$ ,  $t/m^2$ , scheme 1; c) normal stresses,  $\sigma_z$ ,  $t/m^2$ , scheme 2 d) horizontal deformations according to scheme 2.

**3.2 Study of the Properties of Lightweight Concrete with Porous Granular Aggregate**

Results of numerical studies are consistent with characteristics of light alkaline silicate concretes determined by experimental methods (Tables 3, 4).

**Table-3.** Properties of lightweight concrete based on granules of various diameters.

|                                       |     |       |       |
|---------------------------------------|-----|-------|-------|
| Appearance of the granules            |     |       |       |
| Granules' diameter, mm                | 6-8 | 10-12 | 14-16 |
| Bulk density of granules, $kg/m^3$    | 230 | 210   | 195   |
| Compressive strength of concrete, MPa | 5.5 | 4.8   | 4.2   |
| Concrete's structure                  |     |       |       |

**Table-4.** Properties of lightweight concretes with different matrix content.

|  |   |  |   |
|--|---|--|---|
| <b>Appearance of the granules</b>      |  |  |  |
| Matrix content in concrete, %          | 30  | 50   | 70  |
| Density of concrete, kg/m <sup>3</sup> | 420   | 560  | 630   |
| Strength of concrete, MPa              | 4.7   | 5.9  | 7.2   |

Comparative analysis of the properties of concretes obtained on the basis of porous granules of various sizes (Table-3) indicates preference for using particles with diameter from 6 to 8 mm. When a sample of lightweight concrete is loaded, the large-sized granules are more subjected to destructive processes. Lightweight concretes with different ratios between the aggregate and the matrix have been studied (Table-4).

The minimum content of the matrix (30 %) ensures bonding of aggregate granules and creating a large-porous concrete structure with heat-shielding properties. As long as the content of matrix enlarges, its influence on concrete's density and strength increases. When the content of the matrix material is below 30%, non-cohesive molding sand is formed, experiencing deficiency of a binder to bond aggregate grains.

#### 4. CONCLUSIONS

Results of numerical studies of aggregate packing in concrete indicate the advantage of a two-component model built on the fractal principle of a triangle. Compared to the square-based model, the triangular model provides minimal stress and strain within the composite material.

Optimal structure for the two-component model contains 70% of aggregate particles; the matrix substance is at least 30% of composite material's volume.

Analysis of stress isofields shows that the round shape of granules is preferable. Quasi-cylindrical particles with a diameter to length ratio of 1:2 are acceptable. In this case, minimum percentage of matrix increases and it amounts to 40%.

Under regular multi-row distribution of spherical granules, dependence of stress concentration in the composite material on the particle diameter is non-linear. A model containing particles with a diameter of 6 – 8 mm is characterized by minimum concentration of normal and shear stresses.

The results of numerical simulation are confirmed by experimental studies of alkali silicate lightweight concrete with porous granular aggregate. The study of numerical models allows you not only to predict technical characteristics of concrete, but also to carry out targeted

development of effective composite materials with the desired properties.

#### ACKNOWLEDGMENTS

This research is funded by the Science Committee of the Ministry of Education and Science of the Republic of Kazakhstan (Grant No. AP08856219).

#### REFERENCES

- [1] Lu J-X., Shen P., Ali H. A., Poon CS. 2022. Mix design and performance of lightweight ultra high-performance concrete. *Materials & Design*. 216: 110553.
- [2] Li M., Zhou D., Jiang Y. 2021. Preparation and thermal storage performance of phase change ceramsite sand and thermal storage light-weight concrete. *Renewable Energy*. 175: 143-152.
- [3] Miryuk O. A. 2022. Alkaline silicate compositions of porous structure. *ARPN Journal of Engineering and Applied Sciences*. 17(5): 509-517.
- [4] Wang C., Wang H., Liu Z., Chen X., Lv C., Hu Y., Zhu Y. 2018. A novel multifunctional coating prepared by internal and external inhomogeneous modification of porous fillers. *Progress in Organic Coatings*. 119: 57-64.
- [5] García-Cortés V., Estévez D.G., San-José J.T. 2022. Assessment of particle packing models for aggregate dosage design in limestone and EAFS aggregate-based concretes. *Construction and Building Materials*. 328: 126977.
- [6] Lin J., Chen H., Zhang R., Liu L. 2019. Characterization of the wall effect of concrete via random packing of polydispersed superball-shaped aggregates. *Materials Characterization*. 154: 335-343.



- [7] Xu W. X., Lv Z., Chen H.S. 2013. Effects of particle size distribution, shape and volume fraction of aggregates on the wall effect of concrete via random sequential packing of polydispersed ellipsoidal particles. *Physica A: Statistical Mechanics and its Applications*. 392(3): 416-426.
- [8] Jiang Y., Li B., He J., Hernandez A.G. 2022. Properties and microstructure of packing-optimised recycled aggregate concrete with different cement paste or sand contents. *Construction and Building Materials*. 344: 128178.
- [9] Wu F., Yu Q., Brouwers H.J.H. 2022. Mechanical, absorptive and freeze-thaw properties of pervious concrete applying a bimodal aggregate packing model. *Construction and Building Materials*. 333: 127445.
- [10] Chu S. H., Sun C., Poon C.S., Li L. 2021. Effect of natural and recycled aggregate packing on properties of concrete blocks. *Construction and Building Materials*. 278: 122247.
- [11] Andrade G. P., Polisseni G.C., Pepe M., Filho R. D.T. 2020. Design of structural concrete mixtures containing fine recycled concrete aggregate using packing model. *Construction and Building Materials*. 252: 119091.
- [12] Liu S., Minne P., Lulić M., Li J., Gruyaert E. 2021. Implementation and validation of Dewar's particle packing model for recycled concrete aggregates. *Construction and Building Materials*. 294: 123429.
- [13] Pradhan S., Tiwari B. R., Kumar S., Barai S.V. 2019. Comparative LCA of recycled and natural aggregate concrete using Particle Packing Method and conventional method of design mix. *Journal of Cleaner Production*. 228: 679-691.
- [14] Li L.G., Lin C.J., Chen G.M., Kwan A.K.H., Jiang T. 2017. Effects of packing on compressive behaviour of recycled aggregate concrete. *Construction and Building Materials*. 157: 757-777.
- [15] Chen J.J., Guan G.X., Ng P.L., Kwan A.K.H., Chu S.H. 2021. Packing optimization of paste and aggregate phases for sustainability and performance improvement of concrete. *Advanced Powder Technology*. 32(4): 987-997.
- [16] Kondepudi K., Subramaniam K. V. L., Nematollahi B., Bong S. H., Sanjayan J. 2022. Study of particle packing and paste rheology in alkali activated mixtures to meet the rheology demands of 3D Concrete Printing. *Cement and Concrete Composites*. 131: 104581.
- [17] Yang X., Wang M. 2021. Fractal dimension analysis of aggregate packing process: A numerical case study on concrete simulation. *Construction and Building Materials*. 270: 121376.
- [18] Razminia K., Razminia A., Shiryaev V.I. 2020. Application of fractal geometry to describe reservoirs with complex structures. *Communications in Nonlinear Science and Numerical Simulation*. 82: 105068.
- [19] Bala M., Zentar R., Bustingorry P. 2020. Parameter determination of the Compressible Packing Model (CPM) for concrete application. *Powder Technology*. 367: 56-66.
- [20] Klein N. S., Lenz L. A., Mazer W. 2020. Influence of the granular skeleton packing density on the static elastic modulus of conventional concretes. *Construction and Building Materials*. 242: 118086.
- [21] Liu K., Yin T., Fan D., Wang J., Yu R. 2022. Multiple effects of particle size distribution modulus ( $q$ ) and maximum aggregate size ( $D_{max}$ ) on the characteristics of Ultra-High Performance concrete (UHPC): Experiments and modeling. *Cement and Concrete Composites*. 134:104709.
- [22] Wang M., Gao K., Feng Y.T. 2021. An improved continuum-based finite-discrete element method with intra-element fracturing algorithm. *Computer Methods in Applied Mechanics and Engineering*. 384: 113978.
- [23] Liu Y., Feng Y., Zhang R. 2021. A high order conservative flux optimization finite element method for steady convection-diffusion equations. *Journal of Computational Physics*. 425: 109895.
- [24] Miryuk O. A. 2020. Porous grain material based on alkaline silicate composition. *ARPJ Journal of Engineering and Applied Sciences*. 15(6): 737-743.
- [25] Miryuk O., Fediuk R., Amran M. 2021. Foam Glass Crystalline Granular Material from a Polymineral Raw Mix. *Crystals*. 11(12): 1447.